Available online at www.sciencedirect.com
ScienceDirect
Nuclear Instruments and Methods in Physics Research A 570 (2007) 322–329
NUCLEAR INSTRUMENTS & METHODS IN PHYSICS RESEARCH Section A
www.elsevier.com/locate/nima

Localized energy levels generated in Magnetic Czochralski silicon by proton irradiation and their influence on the sign of space charge density ☆

M. Scaringella[a,b,*], D. Menichelli[a,b], M. Bruzzi[a,b], A. Macchiolo[a], C. Piemonte[c], N. Zorzi[c], A. Candelori[d], V. Eremin[e], E. Verbitskaya[e], I. Pintilie[f]

[a]*Department of Energetics, via S. Marta 3, 50139 Florence, Italy*
[b]*INFN, Florence division, via G. Sansone 1, 50019 Sesto Fiorentino, Italy*
[c]*ITC IRST, Via Sommarive, 18 I-38050 Trento, Italy*
[d]*INFN, Padova division, Via Marzolo 8, I-35131 Padova, Italy*
[e]*Ioffe Physical Technical Institute, 26 Polytekhnicheskaya, St. Petersburg 194021, Russian Federation*
[f]*National Institute Material Physics, 105 bis Atomistilor Street, Bucharest-Magurele 077125, Romania*

Available online 2 October 2006

Abstract

The microscopic damage produced in diodes made of n-type Magnetic Czochralski (MCz) silicon by 24 GeV and 26 MeV protons, up to the fluence of $1.3 \times 10^{15}\,cm^{-2}$ 1 MeV equivalent neutrons, has been investigated and results are compared to the damage produced in devices made of standard Floating Zone (STFZ) silicon. It is found by means of Thermally Stimulated Currents (TSC) that the production of a radiation induced charged defect is enhanced in MCz, and might be in part responsible for the differences observed in the two materials at room temperature. The influence of defects on the sign of the space charge density has been studied by current transients at constant temperature $i(T, t)$ and by Transient Current Technique (TCT). Type inversion is not revealed up to the highest investigated fluence. Full depletion voltage V_{dep} measurements versus fluence exhibits a minimum close to $2 \times 10^{14}\,cm^{-2}$ 1 MeV equivalent neutrons; at the same fluence, V_{dep} measured as a function of annealing time changes its initial slope from positive to negative. It is shown by numerical simulations that these features can be accounted by the formation of a double junction, even in absence of type inversion.

PACS: 71.55.Cn; 29.40.Wk; 61.80.Hg; 61.82.Fk

Keywords: Silicon; Radiation damage; Type inversion; Deep levels; TSC; TCT; Current transients

1. Introduction

The CERN Large Hadron Collider luminosity increase up to $10^{35}\,cm^{-2}\,s^{-1}$ is already envisaged [1] and this upgrade will be very challenging for the inner tracking detectors, which will be exposed to a fluence of about $\Phi = 1.6 \times 10^{16}\,cm^{-2}$ 1 MeV equivalent neutrons at a radial distance of 4 cm. Here and in the following, fluences will be often expressed as 1 MeV equivalent neutrons per square centimeter (n/cm^2) [2], to compare samples irradiated with protons of different energy.

The CERN RD48 [3] collaboration already demonstrated the improved radiation tolerance of Diffusion Oxygenated Float Zone (DOFZ) silicon bulk, with respect to Standard Floating Zone silicon (STFZ), related to the higher oxygen concentration of the former material ($[O] \sim 2 \times 10^{17}\,cm^{-3}$). Nowadays, magnetic Czochralski (MCz) [4] ingots suitable for detector production are available. This material has a higher oxygen concentration ($[O] \sim 5 \times 10^{17}\,cm^{-3}$) throughout the ingot and appears to

☆This work has been performed in the frame of the INFN project SMART and of the CERN collaboration RD50.
*Corresponding author. Department of Energetics, via S. Marta 3, 50139 Florence, Italy. Tel.: +39 055 496350; fax: +39 055 4796342.
E-mail address: scaringella@fi.infn.it (M. Scaringella).

0168-9002/$ - see front matter © 2006 Elsevier B.V. All rights reserved.
doi:10.1016/j.nima.2006.09.033

be a very promising material for radiation-tolerant cost-effective detectors. MCz offers the same trapping times [5] and reverse current [6] as STFZ, but has an improved long term annealing, as deduced from measurements on diodes irradiated up to 7×10^{14} n/cm^2, exhibiting a lower stable damage rate [7]. In addition, a proper fabrication process does not induce the formation of thermal donors into the material nor changes the effective doping concentration of the substrate [8,9]. Type inversion has been investigated by TCT and it has been found that MCz does not type invert up to 3×10^{14} n/cm^2 [5]. Similar results have been obtained after 900 MeV electrons irradiation up to a fluence of 6×10^{15} cm^{-2} [10] and low energy protons up to 5×10^{14} n/cm^2 [11].

In n-type STFZ Si, type inversion is usually deduced from the behavior of depletion voltage with fluence, $V_{dep}(\Phi)$, and from the shape of annealing curves $V_{dep}(\Phi, t)$, t being the annealing time spent at constant temperature after the delivery to the sample of the fluence Φ. Close to the fluence of type inversion $V_{dep}(\Phi)$ falls to zero and then starts growing again, while the initial slope of annealing curves dV_{dep}/dt changes its sign from positive to negative. A common feature observed in MCz in many of the cited works is that $V_{dep}(\Phi)$ exhibits a minimum without reaching zero. Anyway, TCT measurements [5] and other tests [10] suggested that this fact should not be considered as an indication of type inversion occurrence. The aims of this paper are to relate the lower stable damage rate in MCz to the radiation induced defect population; to investigate the effect of deep levels on the sign of space charge density; to explain the occurrence of a minimum of $V_{dep}(\Phi)$ and a change in the sign of annealing curves initial slope in absence of type inversion.

2. Samples and experimental methods

2.1. Samples

The bare Czochralski material used in this study ($\langle 1\,0\,0\rangle$, thickness $w = 300\,\mu$m, resistivity $\rho > 500\,\Omega$cm) belongs to MCz 4″ wafers produced by Okmetic Ltd. (Vantaa, Finland). Wafer processing was performed by ITC-IRST (Trento Italy) with sintering at 380 °C and without low-temperature oxidation (LTO). Multiguard diodes used in these studies have a square p^+ implant of $\sim$14 mm^2 active area with a central circular hole on metallization to allow current injection by light. STFZ wafers ($\langle 1\,1\,1\rangle$, $\rho \geqslant 6\,k\Omega$cm) were also produced with a standard process to compare performances. Diodes have been irradiated with 24 GeV protons at the CERN-SPS, and with 26 MeV protons at the cyclotron of the ForschungZentrum in Karlsruhe. A list of the samples used in this study is reported in Table 1.

2.2. Setup

The diodes have been electrically characterized before and after irradiation by means of capacitance versus voltage $C(V)$ measurements [12]. The guard ring of the diodes has always been connected to the ground potential. An Agilent HP4142B was used as voltage source and an Agilent HP4285A as LCR-meter.

Thermally Stimulated Currents (TSC) experiments [13] were carried out using an electrometer (Keithley 6517A) which provides sample bias, low temperature forward injection and current reading. The cooling setup makes use of a liquid helium dewar. The sample holder is mounted on a steel hollow tube which can be lowered inside the dewar at different heights above the liquid surface. The distance between the sample and the liquid helium surface determines the injection temperature. A heating resistor allow one to vary the temperature of the diode. The heating rate was always $\beta \simeq 0.1$ K/s. The temperature sensor is a silicon diode (Lake Shore DT-470-CU11).

In $i(T, t)$ measurements the diode is kept under reverse bias and current transients are measured after a carrier injection produced by a pulsed infrared light emitting diode (wavelength $\lambda \sim 940$ nm). The duration of the excitation pulses was $t_p = 10$ ms. Transients $i(t, T)$ are measured using a custom readout circuit [14], whose output is monitored by a digital oscilloscope (Tektronix TDS520D). Current-Deep Level Transient Spectroscopy (i-DLTS) spectra are obtained from transient samples at time t_1 and t_2 as $S(T) = i(T, t_1) - i(T, t_2)$ during a slow thermal scan ($\beta < 0.07$ K/s).

The TCT setup includes a 500 MHz LeCroy oscilloscope for current response digitizing. Laser pulses with a wavelength 670 nm and 1 ns duration were used for

Table 1
Samples used in this work

Material	Irradiation (protons)	Fluence ($\times 10^{14}$ p/cm^2)	Fluence ($\times 10^{14}$ n/cm^2)	Tests
MCz[a]	24 GeV	4.16	2.50	TSC, $i(T, t)$
MCz[b]	26 MeV	3.68	6.80	$i(T, t)$, i-DLTS
MCz[b]	26 MeV	1.47	2.72	$i(T, t)$
MCz	26 MeV	0.73–5.54	1.35–10.2	$V_{dep}(\Phi, t)$
MCz	24 GeV	5.10–21.7	3.06,13	TCT
STFZ[b]	26 MeV	1.10	2.04	TSC, $i(T, t)$

The fluences, expressed in protons and equivalent 1 MeV neutrons per cm^2, are reported here. TCT measurements have been carried out without annealing. Sample: (a) received a heat treatment of 21 h at 60 °C annealing, samples (b) 6 min at 80 °C.

nonequilibrium carrier generation at the p^+ side of studied detectors.

3. Experimental results

3.1. V_{dep} and annealing measurements

The annealing curves $V_{dep}(\Phi, t)$ of MCz samples irradiated at various fluences of 26 MeV protons are shown in Fig. 1. In general, a short term annealing is followed by a long term one. The end of short term annealing process is approximately indicated by solid markers, while error bars denote the uncertainty related to this evaluation. The uncertainty associated to any voltage value (not shown by error bars for the sake of clearness) is ±20 V. The depletion voltage values at the end of short term annealing are used to draw the plot $V_{dep}(\Phi)$ shown in Fig. 2. It can be seen from Fig. 1 that the initial slope of annealing curves changes from positive to negative as the fluence is raised from 1.36×10^{14} to 5.44×10^{14} n/cm^2. The minimum of $V_{dep}(\Phi)$ occurs in the same fluence range, close to 2×10^{14} n/cm^2. The depletion voltage values measured after 4 min of annealing, as customarily done in the study of STFZ devices, are reported in the figure too. It can be observed that the general trend of $V_{dep}(\Phi)$ curves is not too sensitive to the conventional duration of short term annealing, and that the minimum of these profiles is always found close to 2×10^{14} n/cm^2.

3.2. Thermally stimulated currents

The TSC spectra of two MCz and STFZ samples, irradiated up to a similar equivalent 1 MeV neutron fluence, are shown in Fig 3. Different reverse biases ranging from 10 to 200 V have been used, in order to study the saturation of signal amplitude and to reveal the occurring of Poole Frenkel (PF) effect (a peak shift at lower temperatures as reverse bias

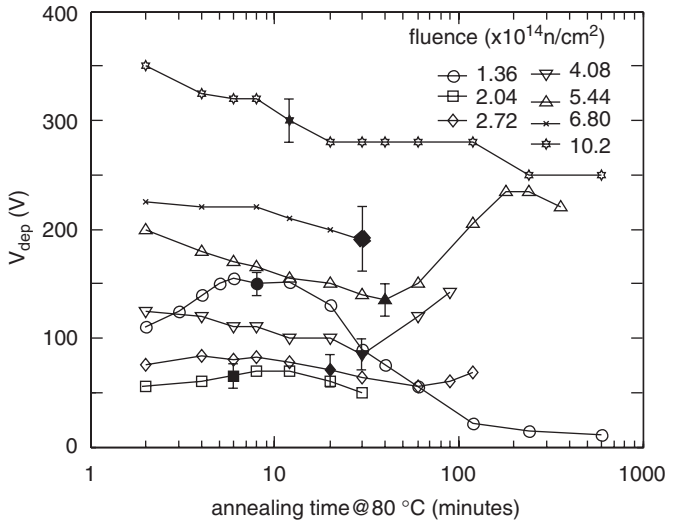

Fig. 1. Annealing curves of MCz samples irradiated at various fluences of 26 MeV protons.

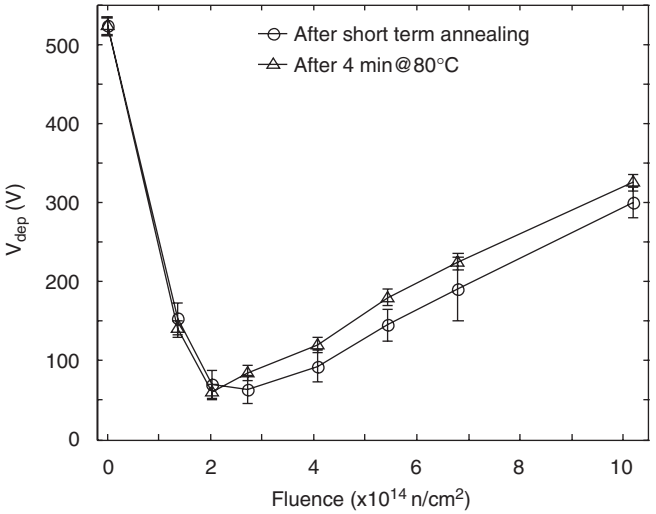

Fig. 2. Evolution with fluence of depletion voltage in MCz samples irradiated by 26 MeV protons. The zero fluence value is the depletion voltage measured before irradiation.

is increased). As a matter of fact, the amplitude of each peak is proportional to the number of emitting levels inside the depleted volume, and saturates when the applied bias is high enough to fully deplete the bulk. The peak observed close to 70 K is due to Vacancy-Oxygen (VO). The interstitial Carbon–substitutional Carbon (C_iC_s) complex, whose formation is strongly suppressed in oxygenated materials [15], contributes to this peak in STFZ materials too. The peaks in the range 40–55 K are due to a group of traps with activation energy around 0.1 eV, formerly detected in γ-ray and ion irradiated diodes [16]. Finally, the peak slightly above 30 K, labeled as "SD", can be attributed to a defect which is charged after emission, since it exhibits PF effect. TSC analysis indicates that thermal donors are not activated in MCz by irradiation [8]. In STFZ the TSC signal saturates with increasing voltage, while in MCz full depletion could not be achieved. From Fig. 3 it is evident that the concentrations [VO] and [SD] are at least 3 and 5 times higher, respectively, in MCz with respect to STFZ. Note that the MCz samples have been measured after hours of reverse annealing; on the contrary, the STFZ sample was measured at the end of beneficial annealing. However, reverse annealing is known to introduce acceptor-like defect and VO is known to anneal out above 300 °C [17], thus the following relationships are expected to hold also in samples with the same annealing history: $[VO]_{MCz}/[VO]_{STFZ} > 3$, $[SD]_{MCz}/[SD]_{STFZ} > 5$.

The fact that [VO] is larger in oxygen rich material is in agreement with former studies on DOFZ silicon [18]. By integrating the area of the SD peak we can evaluate the concentration and the introduction rate of SD. We obtain in MCz: $[SD] \geqslant 1 \times 10^{13}$ cm^{-3} and $[SD]/\Phi$ (1 MeV *neutrons*) $\geqslant 4.7 \times 10^{-2}$ cm^{-1}. This introduction rate is close to the net acceptor introduction rate found by Segneri et al. [7], $\simeq 5.50 \times 10^{-2}$ cm^{-1} and SD is expected to influence substantially the space charge density at room temperature.

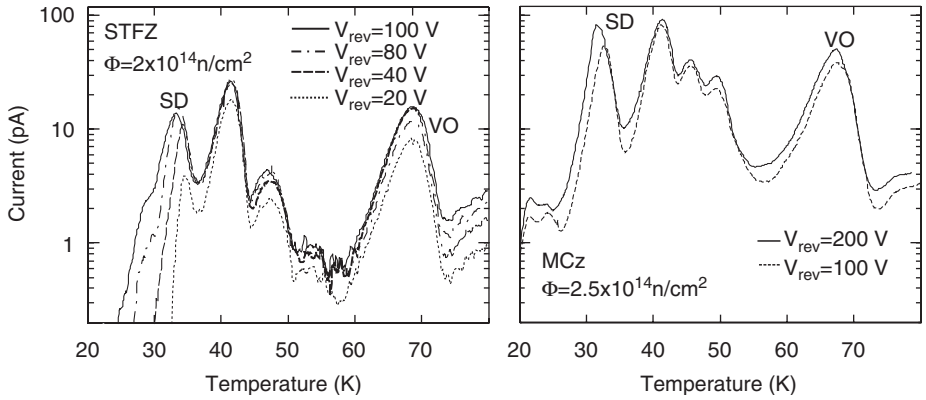

Fig. 3. TSC spectra of the STFZ and MCz samples irradiated with 24 GeV protons up to $\Phi = 2 \times 10^{14}$ n/cm^2 and 26 MeV protons up to $\Phi = 2.5 \times 10^{14}$ n/cm^2, respectively.

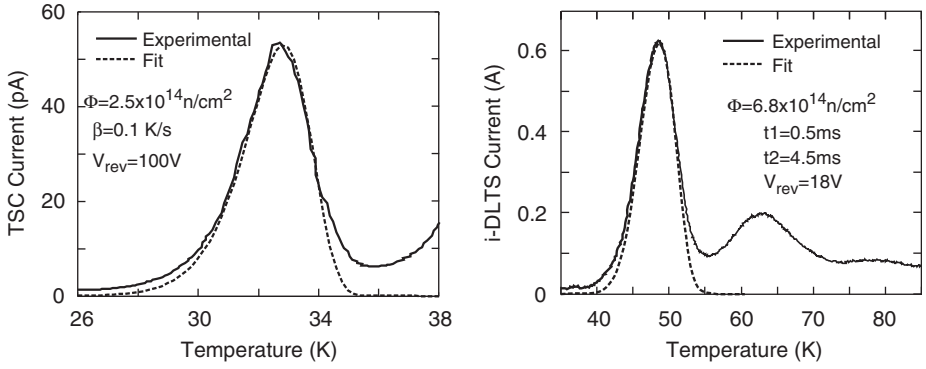

Fig. 4. Fit of TCS and *i*-DLTS signals from SD level recorded in MCz samples.

A detail of SD signal in TSC and *i*-DLTS spectra emission from SD, recorded in the MCz sample, is shown in Fig.4. The zero field activation energy $E_a = 85 \pm 15$ meV and the apparent cross-section $\sigma_a \sim 10^{-14}$ cm^2 determine the best fit of the lineshapes, as shown in the plots [19].

3.3. Current transients at constant temperature

Current transients at constant temperature $i(T,t)$ have been used to determine the inversion of the investigated samples. A nonmonotonic $i(T,t)$ profile indicates the occurring of space charge sign inversion (SCSI) [20]. Current transients were recorded during the emissions $V_2^{-/0}$ and $I^{0/-}$. Using a timescale of ≈ 1 ms these emissions occur close to $T = 250$ and 300 K, respectively. A clear bump in transient profile is measured during $V_2^{-/0}$ in all the samples, indicating that a SCSI takes place during V_2 discharge and that the materials are not inverted between $V_2^{-/0}$ and $I^{0/-}$ emissions. The transients measured on the MCz sample irradiated at $\Phi = 2.72 \times 10^{14}$ n/cm^2 are shown in Fig. 5. On the contrary, current transients measured close to room temperature are very different in the two materials, as shown in Fig. 6. In STFZ the transients are nonmonotonic and exhibit a bump, indicating that SCSI occurs during $I^{0/-}$ emission. A similar feature is not observed in MCz samples, even if their shape is distorted and far from exponential. Thus we can conclude that, at room temperature, the STFZ sample is

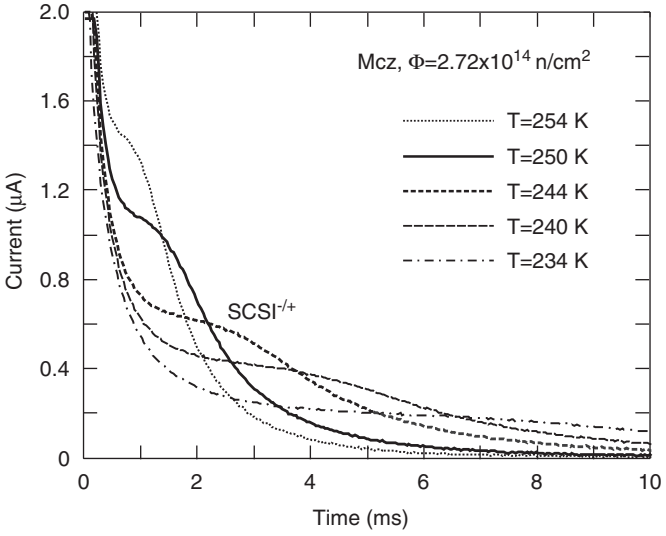

Fig. 5. Current transients measured in MCz sample irradiated at $\Phi = 2.72 \times 10^{14}$ n/cm^2 at temperatures ranging from $T = 234$ to 254 K; the SCSI$^{-/+}$ during $V_2^{-/0}$ emission can be observed.

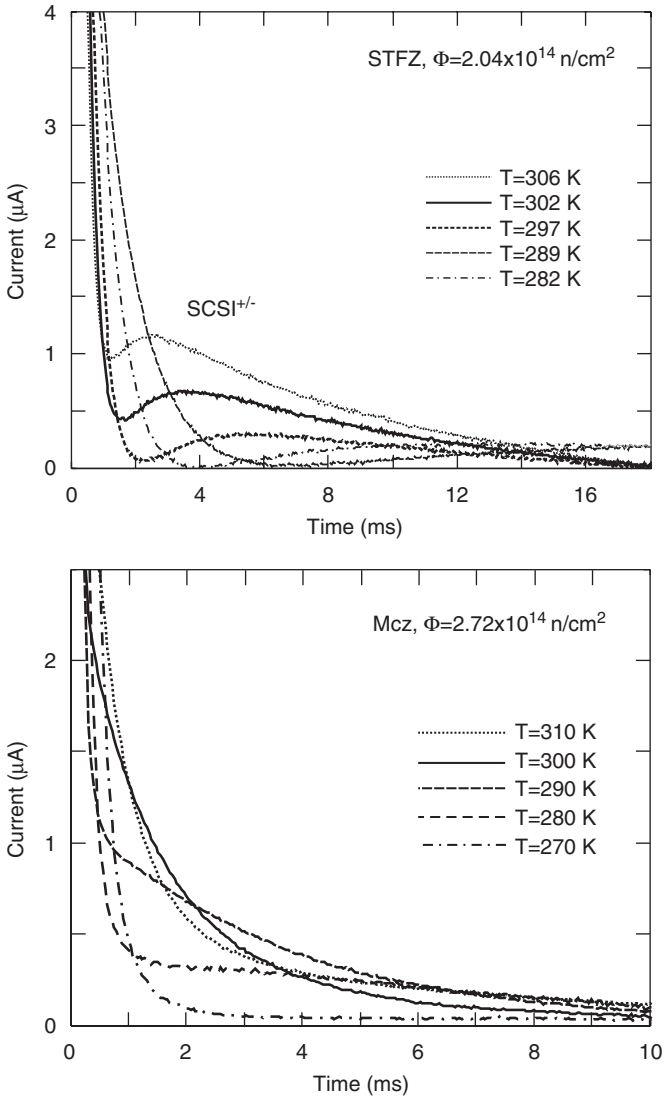

Fig. 6. Current transients measured in a STFZ diode (irradiated at $\Phi = 2.04 \times 10^{14}\,\mathrm{n/cm^2}$) and in a MCz diode (irradiated at $\Phi = 2.72 \times 10^{14}\,\mathrm{n/cm^2}$) close to $T = 300\,\mathrm{K}$. The $\mathrm{SCSI}^{+/-}$ in STFZ during $I^{0/-}$ emission is evidenced.

inverted while the MCz samples are not. Similar results have been obtained up to $\Phi = 6.8 \times 10^{14}\,\mathrm{n/cm^2}$.

3.4. Transient current techniques

Two MCz samples irradiated by proton at the fluences of 3.06×10^{14} and $1.3 \times 10^{15}\,\mathrm{n/cm^2}$ have been studied using TCT method. The current pulse recorded in the sample irradiated to $1.3 \times 10^{15}\,\mathrm{n/cm^2}$ is shown in Fig. 7. At low bias voltage, the shape of TCT signal exhibits a single peak for all three detectors. As the bias is increased, the signal shape becomes doubly peaked. This double-peak shape originates from the electric field profile specific for heavily irradiated silicon detectors. This profile has strong electric field on both p^+ and n^+ sides denoting the appearing of the double junction effect [21]. The measured pulse shapes have been fitted according to the procedure described in Ref. [22] in order to determine the electric field distribution inside the sample. The results (Fig. 7, right) show that, even at this fluence level, the dominant junction is still on the p^+ side. This suggests that, in agreement with $i(T,t)$ measurements, the sample is not inverted.

Samples studied by TCT did not receive annealing. However, beneficial annealing is equivalent to a process of donor creation or acceptor removal, and would not be able to produce type inversion of the sample.

4. Discussion

TCT and $i(T,t)$ analyses confirms that MCz samples are not type inverted at room temperature up to the fluence of $\Phi = 1.3 \times 10^{15}\,\mathrm{n/cm^2}$. Space charge density in the STFZ sample becomes negative during the transition $I^{0/-}$; on the contrary, the space charge density in MCz remains always positive after $V_2^{-/0}$ emission. This is consistent with a suppressed generation of I defect in oxygen rich silicon, already observed by other authors [18], and with the enhanced generation of charged defects in MCz, revealed by TSC, if they were donors. Anyway, it is necessary to understand why, close to the fluence of $2 \times 10^{14}\,\mathrm{n/cm^2}$, a minimum is observed in $V_{\mathrm{dep}}(\Phi)$ and a change in initial slope occurs in annealing curves $V_{\mathrm{dep}}(\Phi,t)$. These phenomena can be explained in terms of double junction effect (DJ), as suggested by the fact that, according to TCT results, a double junction is formed in MCz even in absence of type inversion. This situation is different from the case of STFZ, in which the fluence of double junction formation Φ_0 is higher than the type inversion fluence Φ_i. For instance, in neutron-irradiated high resistivity STFZ samples $\Phi_i \simeq 10^{13}\,\mathrm{cm^{-2}}$, while $\Phi_0 \simeq 10^{14}\,\mathrm{cm^{-2}}$ [23]. We refer here to ''type inversion'' and not to ''space charge sign inversion'' in order to avoid the ambiguities arising from the formation of two depleted regions with different space charge sign. Type inversion may be determined by Hall effect measurements. In general, the fluences at which SCSI and type inversion occur are not exactly the same.

Consider a MCz $p^+/n/n^+$ diode irradiated at a fluence $\Phi_0 < \Phi < \Phi_i$. Let N_1 and N_2 be the effective doping concentrations close to p^+ and n^+ implants, respectively, such as the space charge densities are $\rho_1 = eN_1$, $\rho_2 = -eN_2$, e being the elementary charge. We will treat the two junctions as bipolar junctions with uniform doping concentration. However, this is only a rough approximation, because ρ is determined by three components:

(1) residual dopant (let N_{D} denote its concentration);
(2) radiation induced donors and acceptors (with net concentration $N_{\mathrm{RD}} - N_{\mathrm{RA}}$) such as SD and I defect;
(3) deep traps such as C_iO_i, V_2, which are neutral in the bulk but might remain charged close to implants due to band-bending. Only a fraction $N_t(x)$ of total deep traps concentration N_{T} remains charged close to implants, producing a nonuniform contribution to space charge density. It allows for the formation of the double

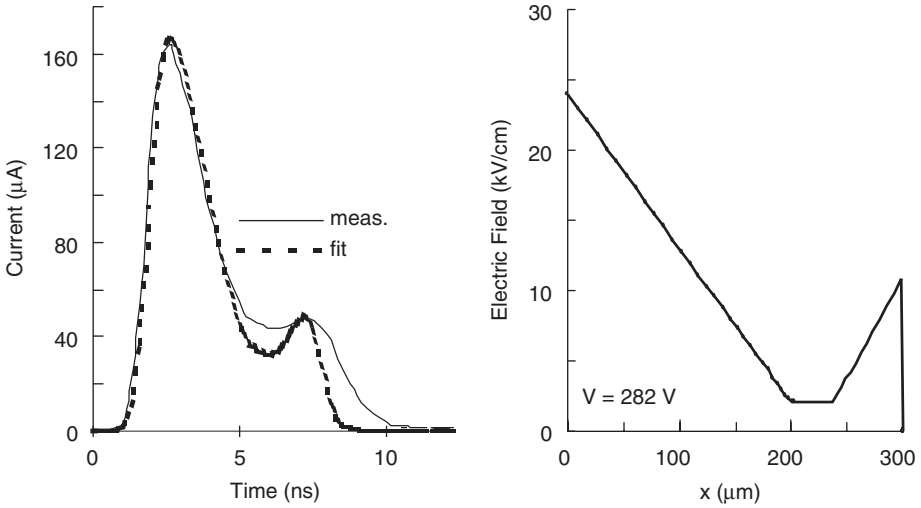

Fig. 7. Left plot: the TCT measured in MCz sample irradiated at 1.3×10^{15} 1 MeV n/cm^2, using $V_{rev} = 282$ V. Right plot: electric field profile as reconstructed from current pulse fitting.

junction [24], and makes its behavior quite different from a bipolar junction with uniform doping. Vacancy clusters are not expected to play a key role after proton irradiation [25].

In our situation, the bulk is not inverted and N_1 is due mainly to the contribution from residual phosphorus and from radiation induced donors and acceptors. On the contrary, N_2 is due mainly to deep electron traps, such as V_2. In this picture, a cut off fluence Φ_0 for DJ formation arises from the fact that the second junction (with negative space charge density) can exist only if: $N_T > N_D + N_{RD} - N_{RA}$.

It is convenient to replace the depletion voltage with the quantity $C = 2\varepsilon V_{dep}/(ew^2)$, which has the dimension of a concentration. Here ε is the absolute silicon dielectric constant. In the case of a single junction with doping concentration N, we would get $C = N$. The problem of finding the form of $C(N_1, N_2)$ would require extensive numerical simulation to solve transport equations. As a first attempt, we look for a function which satisfies some basic requirements:

(1) *Symmetry*: $C(N_1, N_2) = C(N_2, N_1)$. This is a rough simplification because, as discussed above, the two junctions are created by very different kinds of localized states.
(2) $C \sim N_1$ if $N_2 \sim 0$ (in this case we have a single junction) and if $N_1 \gg N_2$ (in which case the first junction dominates over the second).
(3) If $N_1 \sim N_2$ the depletion voltage must be lower than the voltage level that would be necessary to deplete a single junction diode. In particular, due to former symmetry hypothesis, if $N_1 = N_2$ we must have $C = N_1/2 = N_2/2$. This is the phenomenon which really produces a minimum in $V_{dep}(\Phi)$.

We will adopt the model function: $C(N_1, N_2) = (N_1 + N_2) - 3N_1N_2/(N_1 + N_2)$. The limit of this simple model is not due to the arbitrariness of this function, but mainly to the symmetry requirement.

In order to predict in a simple way the effect of irradiation, we model the evolution of $N_{1,2}(\Phi)$ as

$$\begin{cases} N_1(\Phi) = N_{10} - b_1\Phi = b_1(\Phi_i - \Phi) \\ N_2(\Phi) = b_2(\Phi - \Phi_0). \end{cases} \quad (1)$$

Here we have introduced two (positive) rates $b_{1,2}$. N_{10} is the doping level before irradiation and $\Phi_i = N_{10}/b_1$ is the fluence of type inversion. Eq. (1) depends on four parameters $(b_1, b_2, \Phi_i, \Phi_0)$, but the shape of C function is sensitive only on their relative values. To evidence this we normalize C to its zero fluence value, thus obtaining

$$\begin{cases} n_1(\phi) = (1 - \phi) \\ n_2(\phi) = s(\phi - \phi_0). \end{cases} \quad (2)$$

Here $s = b_2/b_1$ is the ratio of defect introduction rates in the two junctions, while all the fluences are normalized to the fluence of type inversion: $\phi = \Phi/\Phi_i$. If we substitute Eq. (2) inside $C(N_1, N_2)$ in place of $N_{1,2}$, we obtain a function $C(\phi)$ which has the same shape of $V_{dep}(\Phi)$. The value of ϕ_0 merely stretches C along ϕ axis, and we choose it to be $\phi_0 = 0.1$. As an example, the curves which are obtained with s spanning a wide range of values are shown in Fig. 8. In agreement with measurements, the minimum value of C can be substantially higher than zero and generally occurs at a fluence lower than that of type inversion.

The effect of short term annealing, equivalent to a net acceptor annihilation, can be modeled in a similar fashion:

$$\begin{cases} N_1'(\Phi, t) = N_1'(\Phi, 0) + a_1 t \\ N_2'(\Phi, t) = N_2'(\Phi, 0) - a_2 t. \end{cases} \quad (3)$$

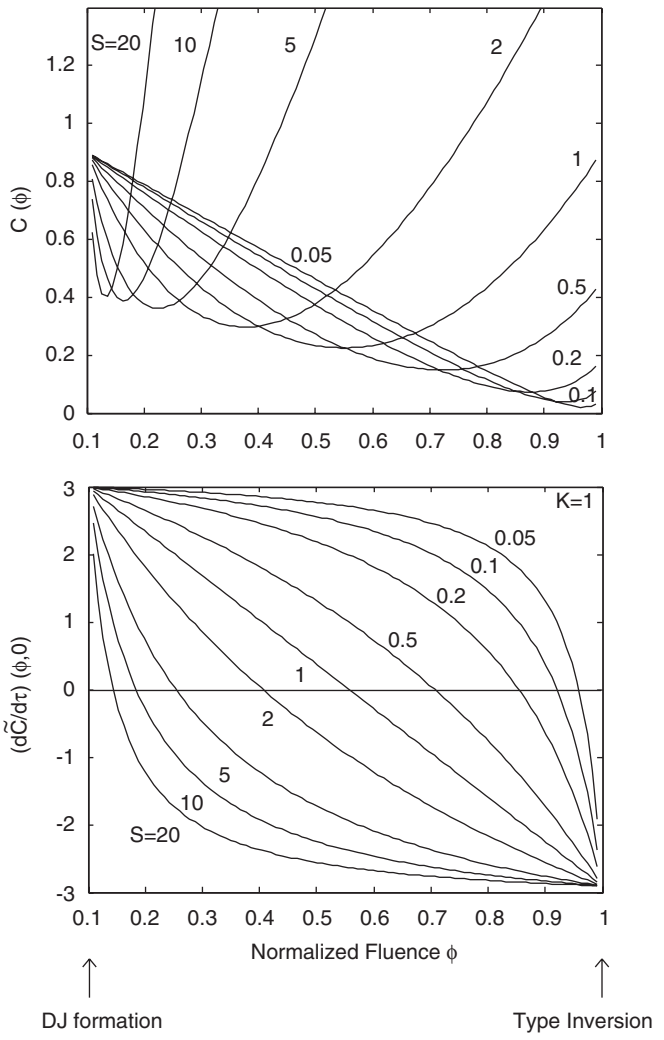

Fig. 8. Simulation results. Evolution of $C(\phi)$ (upper plot) and initial slope of the function $\tilde{C}(\phi,\tau)$. We used $\phi_0 = 0.1$ and $k = a_2/a_1 = 1$. All the fluences are normalized to the fluence Φ_i of type inversion. Different curves correspond to different values of $s = b_2/b_1$.

Here $a_{1,2}$ are two (positive) rates. It is convenient to divide right and left hand sides of these equations by $N_2'(\Phi,0)$, thus obtaining the ratio $r = N_1'(\Phi,0)/N_2'(\Phi,0) \approx n_1(\phi)/n_2(\phi)$; then we rescale time axis by introducing the new variable $\tau = a_1 t/N_2(\Phi,0)$. At the end we get $(k = a_2/a_1)$:

$$\begin{cases} n_1'(\phi,\tau) = r + \tau \\ n_2'(\phi,\tau) = 1 - k\tau. \end{cases} \quad (4)$$

After having replaced by these expressions (N_1, N_2) in $C(N_1, N_2)$, a set of curves $\tilde{C}(\phi,\tau)$, having the same shape of annealing curves $V_{\text{dep}}(\Phi,t)$, are obtained. The initial slope of these curves, $(\mathrm{d}\tilde{C}/\mathrm{d}\tau)(\phi,0)$, calculated with $k = 1$, is shown in the bottom of Fig. 8. In agreement with experimental results, the fluence at which the initial slope of $\tilde{C}$ changes its sign is very close to the fluence of C minimum, and may be significantly lower than the fluence of type inversion. The effect of having $k \neq 1$ is just to shift the fluence at which $\tilde{C}$ changes its slope with respect to the fluence corresponding to the minimum of C.

5. Conclusions

Microscopic damage produced by 24 GeV and 26 MeV protons, up to the equivalent 1 MeV neutrons fluence of 1.3×10^{15} n/cm^2 in n-type high resistivity Magnetic Czochralski (MCz) Si, has been investigated. The analysis has been carried out also on companion diodes made of standard Floating Zone (STFZ) silicon, in order to compare the radiation damage in the two materials. The relationship between microscopic disorder and type inversion has been studied, and the particular features of depletion voltage and annealing experiments have been discussed in terms of radiation induced deep levels.

Localized energy levels produced by radiation have been studied by TSC spectroscopy in the temperature range 10−80 K. It has been found that no thermal donors are activated in MCz; however a radiation induced charged defect has been found in MCz in a concentration at least five time higher than in STFZ. This energy state gives a substantial contribution to the space charge density at room temperature. In particular, if this level was a donor, it could be responsible for the lower stable damage rate measured in MCz.

The influence of defects on the sign of the space charge density has been investigated by current transients at constant temperature $i(T,t)$ and by Transient Current Technique (TCT). Type inversion is not revealed in MCz up to the highest investigated fluence. Thus the minimum measured in depletion voltage $V_{\text{dep}}(\Phi)$ close to 2×10^{14} cm^{-2} and the change in initial slope of annealing curves $V_{\text{dep}}(\Phi,t)$ in the same fluence range cannot be considered as a signature of type inversion. It is then shown by means of numerical simulations that these feature of depletion voltage measurements can be explained in terms of the formation of a double junction at a fluence lower than type inversion one.

Further TCT investigations on MCz samples irradiated by protons at fluences higher than 1×10^{15} n/cm^2 and by neutrons have been carried out and data analysis is presently under way.

Acknowledgments

Authors would like to thank D. Creanza, N. Manna and V. Radicci, of INFN Bari, and A. Messineo of INFN Pisa, for suggestions and helpful discussions. Moreover, we are grateful to I. Ilyashenko of Ioffe Physical Technical Institute for his assistance during TCT measurements.

References

[1] F. Gianotti, et al., hep-ph/0204087.
[2] G. Lindstroem, Nucl. Instr. and Meth. A 512 (2003) 30.
[3] The RD48 Collaboration, CERN LHCC 2000-009.

[4] V. Savolainen, et al., J. Cryst. Growth 243 (2002) 243.
[5] A.G. Bates, M. Moll, Nucl. Instr. and Meth. A 555 (2005) 113.
[6] G. Pellegrini, M. Ullán, J.M. Rafí, C. Fleta, F. Campabadal, M. Lozano, Nucl. Instr. and Meth. A 552 (2005) 27.
[7] G. Segneri, et al., accepted for publication on Nucl. Instr. and Meth. A.
[8] M. Bruzzi, et al., Nucl. Instr. and Meth. A 552 (2005) 20.
[9] G. Pellegrini, J.M. Rafi, M. Ullan, M. Lozano, C. Fleta, F. Campabadal, Nucl. Instr. and Meth. A 548 (2005) 355.
[10] S. Dittongo, L. Bosisio, D. Contarato, G. D'Auria, E. Fretwurst, J. Härkönen, G. Lindström, E. Tuovinen, Nucl. Instr. and Meth. A 546 (2005) 300.
[11] J. Härkönen, et al., Nucl. Instr. and Meth. A 541 (2005) 202.
[12] A. Chilingarov, IV and CV measurements in Si diodes, RD50 Technical Note RD50-2003-03, available at ⟨www.cern.ch/rd50⟩.
[13] M.G. Buehler, Solid State Electron 15 (1972) 69.
[14] D. Menichelli, M. Scaringella, M. Bruzzi, Phys. Rev. B 70 (2004) 195209.
[15] J. Stahl, E. Fretwurst, G. Lindstrom, I. Pintilie, Nucl. Instr. and Meth. A 512 (2003) 111.
[16] M. Scaringella, D. Menichelli, A. Candelori, R. Rando, M. Bruzzi, IEEE Trans. Nucl. Sci. NS-53 (2006) 11.
[17] G.D. Watkins, Mater. Sci. Semicond. Proc. 3 (2000) 227.
[18] I. Pintilie, E. Fretwurst, G. Lindstroem, J. Stahl, Appl. Phys. Lett. 82 (2003) 2169.
[19] J.L. Hartke, J. Appl. Phys. 39 (1968) 4871.
[20] D. Menichelli, M. Scaringella, S. Miglio, M. Bruzzi, Z. Li, E. Fretwurst, I. Pintilie, Nucl. Instr. and Meth. A 530 (2004) 139.
[21] V. Eremin, Z. Li, I. Iljashenko, Nucl. Instr. and Meth. A 360 (1995) 458.
[22] E. Verbitskaya, V. Eremin, I. Ilyashenko, Z. Li, J. Härkönen, E. Tuovinen, P. Luukka, Nucl. Instr. and Meth. A 557 (2006) 528.
[23] M. Bruzzi, IEEE Trans. Nucl. Sci. NS-48 (2001) 960.
[24] Z. Li, H.W. Kraner, J. Electron. Mater. 21 (1992) 7.
[25] M. Huhtinen, Nucl. Instr. and Meth. A 491 (2002) 194.